A Model for the ΔE Effect in Magnetostrictive Transducers

Marcelo J. Dapino[a*], Ralph C. Smith[b], Alison B. Flatau[a]

[a] Department of Aerospace Engineering and Engineering Mechanics, Ames, IA 50011
[b] CRSC, Department of Mathematics, North Carolina State University, Raleigh, NC 27695

ABSTRACT

Changes in elastic moduli of between 0.4-18% are common in ferromagnetic materials such as nickel and iron when their magnetization is changed. However, extremely large moduli changes of up to 160% are observed in the rare earth-iron compounds R-Fe$_2$, which can be advantageously utilized in design of smart structure systems. A nonlinear, hysteretic and magnetoelastically coupled model is presented and used to quantify the changes in resonance frequency exhibited by a loaded magnetostrictive transducer under varied bias magnetizations. The model is constructed in three steps. In the first, the magnetization of the magnetostrictive material is quantified by considering the energy lost to hysteresis as the magnetic field and operating stresses vary. In the second step, a quartic law is used to quantify the magnetostriction arising from domain rotations in the material. The material response, of the type found in linearly elastic solids, is considered in the final step by means of force balancing in the magnetostrictive material. This yields a PDE system with magnetostrictive inputs and boundary conditions given by the transducer-load characteristics. The solution to the PDE system provides displacements and accelerations in the material. Fast Fourier Transform (FFT) analysis is then used to quantify the frequency-domain acceleration response from which the transducer's resonance frequency is calculated. Model results are compared with published experimental data.

Keywords: ΔE effect, magnetostriction, transducers, Terfenol-D

1 INTRODUCTION

We address the modeling of stiffness changes which occur when magnetostrictive materials are exposed to DC magnetic fields. The interest in magnetostrictive materials for applications involving high power actuation and sensing has increased considerably in recent years. This is due to the availability of highly capable transducer materials which deliver strains on the order of 10^{-3} and forces of several kN. While recent advances in the modeling of magnetostrictive devices have facilitated better control laws [1] and design optimization tools [2], information on the stiffness variations occurring during operation of these devices is still insufficient. Such stiffness changes can be used, for instance, in adaptive vibration absorbers to tune the resonance frequency of the magnetostrictive resonator in relation to that of the host structure. Notably, experimental evidence suggests that the magnetostrictive absorber's damping signature may be virtually unaffected by the resonance frequency shift [3].

Several factors complicate the ability to ascertain the elastic modulus of magnetostrictive materials. In these materials, the strain is produced by two contributions: (i) an elastic component of the type occurring in any substance, magnetic or not, and (ii) a magnetoelastic component, due to the reorientation of magnetic moments produced by magnetic fields or stresses. Employing the classical definition of elastic modulus as the ratio between stress and strain in the material, it is inferred that the elastic modulus of magnetostrictive materials (or in a general sense of materials with actively induced strains) is a rather complicated property. The elastic modulus of magnetostrictive materials is a function of mechanical properties as much as it is a function of magnetic properties.

To illustrate the dependency of the elastic modulus on magnetoelastic properties, linearized expressions of the generalized Hooke's law for changes in strain ($\Delta\varepsilon$) and changes in magnetic induction (ΔB) are considered. Denoting by E^H, μ^σ and d the components of the elastic modulus under constant magnetic field, the constant-stress

---

*(Correspondence)- Email: marcelod@iastate.edu; Telephone: 515-294-0084; Fax: 515-294-3262

permeability and the longitudinal piezomagnetic constant, respectively, the isothermal piezomagnetic equations are

$$\Delta\varepsilon = (1/E^H)\,\Delta\sigma + d\,\Delta H, \tag{1}$$

$$\Delta B = d\,\Delta\sigma + \mu^\sigma\Delta H, \tag{2}$$

where ΔH is the applied field and $\Delta\sigma$ is the stress variation.

Following procedures proposed by Clark [4, 5], equations (1)-(2) are rearranged by eliminating ΔH and $\Delta\sigma$, respectively, which yields

$$\Delta\varepsilon = (1/E^H)\left[1 - d^2 E^H/\mu^\sigma\right]\Delta\sigma + (d/\mu^\sigma)\,\Delta B, \tag{3}$$

$$\Delta B = d\,E^H\,\Delta\varepsilon + \mu^\sigma\left[1 - d^2 E^H/\mu^\sigma\right]\Delta H. \tag{4}$$

It then follows that the expression between square brackets in equation (3) represents the inverse of the constant-induction elastic modulus E^B (magnetically blocked condition),

$$1/E^B = (1/E^H)\left[1 - d^2 E^H/\mu^\sigma\right], \tag{5}$$

whereas the expression between square brackets in equation (4) represents the constant-strain permeability μ^ε (mechanically blocked condition),

$$\mu^\varepsilon = \mu^\sigma\left[1 - d^2 E^H/\mu^\sigma\right]. \tag{6}$$

It is standard practice in magnetostrictive transducer analysis to define a magnetomechanical coupling factor k which quantifies the coupling between the magnetic and elastic systems. In a lossless transducer, k^2 represents the ratio of magnetic energy which can be converted to elastic energy per cycle (actuator mode), or conversely, the fraction of stored elastic energy which can be converted to magnetic energy per cycle (sensor mode). In the low-signal, linear regime where equations (1)-(2) hold, k^2 can be expressed in terms of the magnetoelastic properties E^H, μ^σ and d. This is accomplished by considering the energies in the elastic and magnetic systems, giving [4]

$$k^2 = d^2\,E^H/\mu^\sigma. \tag{7}$$

Typical values of k are 0.3 for nickel, 0.7-0.8 for Terfenol-D and up to 0.95 for the R-Fe$_2$ amorphous alloys.

The magnetomechanical coupling factor can be used to establish a relation between the short circuit modulus E^B with the open circuit or magnetically free modulus E^H, and between the mechanically blocked permeability μ^ε with the mechanically free permeability μ^σ. Substitution of equation (7) into (5) and (6) yields

$$E^B = E^H/(1 - k^2), \quad \mu^\varepsilon = \mu^\sigma\,(1 - k^2).$$

Recognizing that $k = 0$ represents no transduction and $k = 1$ represents perfect transduction between the magnetic and elastic states ($0 \leq k \leq 1$), it is inferred that efficient magnetostrictive materials must necessarily be soft and have low permeabilities.

To motivate the model and corresponding numerical results presented in this paper, we now focus the attention on the two moduli of elasticity, E^H and E^B. It is noted that the latter represents the stiffest material condition, which occurs when all available magnetic energy has been transduced into elastic potential energy. As energy is transferred from the elastic to the magnetic system, the effective modulus decreases progressively following the trend $E^H = E^B(1-k^2)$, until the softest magnetoelastic state E^H is achieved. This stiffness variation is interpreted through consideration of the resonant frequencies shown in Figure 1. It is noted that the first mode resonance frequency of a longitudinal resonator is $f = (1/2\pi)\left[(K_d + K_t)/M_e\right]^{1/2}$, where $K_d = EA/L$ (A = area, L = length) is the stiffness of the magnetostrictive driver, K_t is the stiffness of relevant prestress components and M_e is the effective dynamic mass of the system. Thus, f is proportional to $E^{1/2}$, which implies that two resonance frequencies can be defined, one at constant induction and the other at constant field. Methods for determining resonance include electrical impedance analysis and wave propagation techniques [6].

While the variation between the moduli E^B and E^H is significant, particularly at low DC magnetic fields, the focus of this paper is on the field-induced hardening or ΔE effect,
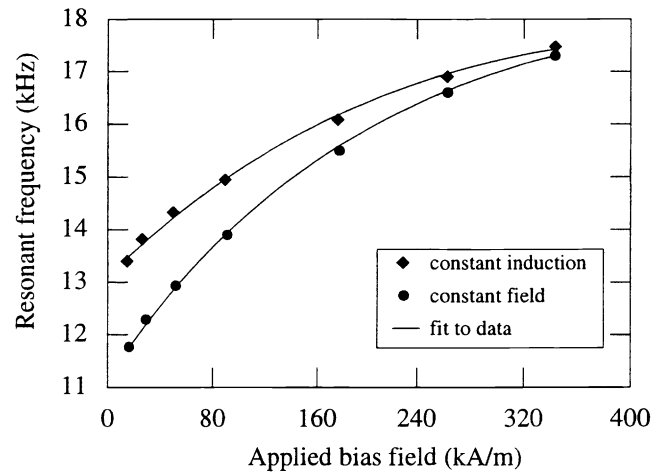
$$\Delta E/E_0 \equiv (E - E_0)/E_0, \tag{8}$$

175

Figure 1: Resonant frequency at constant magnetic induction (E^B) and constant magnetic field (E^H) versus magnetic bias. (From [7]).

in which E is the elastic modulus at applied DC magnetic field H and E_0 is the elastic modulus at zero field. It is emphasized that although the variation between moduli can be used as a design tool in applications (see, for instance, reference [8] regarding piezoelectric materials whose moduli are adjusted with variable shunt resistances), the ΔE effect involves substantially larger stiffness variations.

Published experimental results regarding the ΔE effect in Terfenol-D are drawn upon and used as a basis for evaluation of the model results presented here. Changes in elastic modulus of up to $\Delta E/E_0 = 161\%$ have been reported by Clark and Savage in $Tb_{.28}Dy_{.72}Fe_2$ samples subjected to saturation magnetic fields of 4.3 kOe [9]. The corresponding frequency increase for this composition was 61%. The reported stiffness changes are highly sensitive to material composition and operating conditions, particularly stress [10]. We point out that the biggest stiffness effects achievable with conventional metals such as Ni or Fe are of only 0.4-18%. Consequently, significant variations should be expected.

Data from ref. [9] on the elastic modulus and ΔE effect versus magnetic field of $Tb_{.3}Dy_{.7}Fe_2$ are shown in Figure 2(a). The fit to data shown in the figure, taken directly from the reference, suggests that the stiffness change is positive at all bias field values. However, experimental results on Terfenol-D and other materials have been reported which suggest that negative ΔE effects may occur at low bias fields due to magnetization jumping [11, 12]. Data from [13] supporting this observation are shown in Figure 2(b).

Because the largest effects were originally found in soft materials with large magnetostrictions, the ΔE effect has been generally associated with domain wall motion. In the R-Fe_2 compounds, however, the moduli continue to change even far above technical saturation, which excludes domain wall motion as a major contributor to the ΔE effect. Citing Clark [4], the major source of field dependency for the modulus is the intrinsic softening of the lattice (upon reduction of the field from saturation) due to local magnetoelastic interactions. Thus a transducer model capable of addressing the coupling between the magnetic and elastic systems ought to prove viable for modeling the ΔE effect. If, in addition, the model is capable of characterizing the nuances of magnetic hysteresis and magnetostrictive nonlinearities, even greater accuracy is possible.

A model formulation which addresses the above issues has been developed recently [13, 14, 15]. This model has been employed to characterize both magnetostrictive actuators [15] and sensors [16]. The model is summarized in Section 2 of this paper, in the context of a transducer consisting of a cylindrical magnetostrictive driver, a surrounding excitation solenoid, a closed magnetic circuit and a preload mechanism. In Section 3, the model is used to quantify the first-mode resonance frequency of the transducer when the magnetostrictive rod is magnetized with a DC field H_0. Specifically, the rod is magnetized by passing current through the solenoid and mechanically excited with an impact applied on one end. The coupled magnetization, accelerations and stresses produced as a consequence of the impact are quantified, and Fast Fourier Transformations (FFT) are used to compute frequency-domain acceleration responses. The transducer's resonance frequency f_r is then calculated from the acceleration per frequency curve. Finally, the value of the resonance frequency is plotted against the corresponding value of the DC magnetic field.
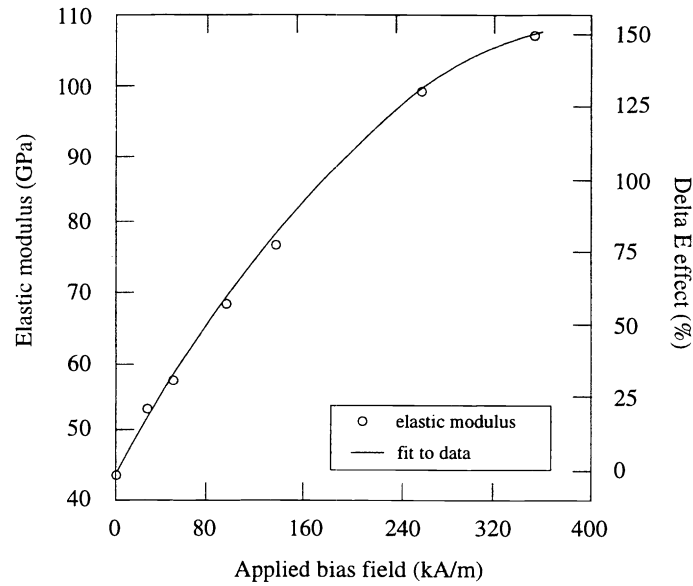
(a)
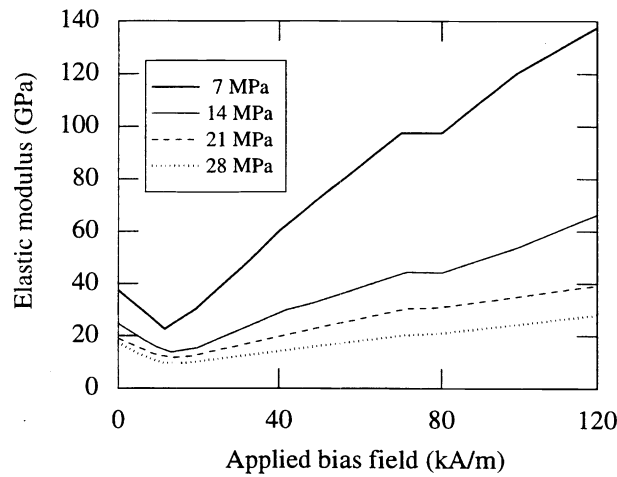
(b)

Figure 2: (a) Elastic modulus and ΔE effect versus bias magnetic field of $Tb_{.3}Dy_{.7}Fe_2$, after [9], and (b) elastic modulus at various prestress levels, after [13].

2   TRANSDUCER MODEL

The model is illustrated in the context of the transducer design shown in Figure 3, which is typical of control applications and illustrates the primary components needed to fully utilize the magnetostrictive transducer capabilities. These components are a magnetostrictive rod, an excitation solenoid which provides the bias magnetization, a prestress mechanism consisting of a bolt and a spring washer, a permanent magnet which is used in conjunction with the solenoid to fine-tune the bias magnetization and magnetic couplers.

The model is constructed in three steps. In the first, we consider the magnetization M of the magnetostrictive rod under an externally applied magnetizing field H_0 and a stress field σ. The field-induced component of magnetization is quantified with the mean field model of ferromagnetic hysteresis originally proposed in [17]. The stress-induced component of magnetization is modeled with a law of approach to the anhysteretic magnetization as presented in [18].
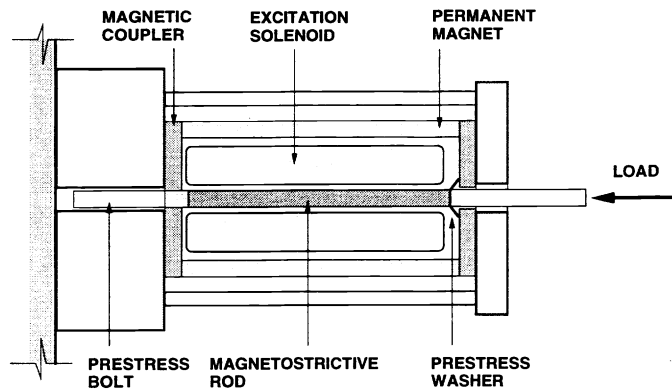
Figure 3: Cross section of the prototypical Terfenol-D transducer employed for model development.

The two components considered together provide a magnetization model based on the energy dissipated when domain walls attach to and detach from inclusions in the material.

The second step involves the characterization of the magnetostriction λ produced when the magnetostrictive rod is magnetized. This is accomplished through a phenomenological model consisting of an even-terms series expansion depending on M. While λ includes the active contribution to the strain arising from the rotation of magnetic moments, it does not account for the material response of the kind found in linearly elastic materials.

These elastic effects are modeled in the third step, through consideration of force balancing in the magnetostrictive rod in the form of a PDE equation which includes the intrinsic magnetostriction, system compliance, internal damping and boundary conditions associated with the transducer-load characteristics. The solution to this PDE provides the rod displacements, total strains and corresponding accelerations.

2.1 Magnetization of Magnetostrictive Element

Magnetostrictive transducers are customarily operated with a magnetic bias. This facilitates operation over the region of maximum output per input in the M-H and ε-H curves and leads to bidirectional operation around the bias point. The magnetization changes are thus assumed to be dictated by the expression

$$\frac{dM}{dt} = \left(\frac{\partial M}{\partial H}\right)\frac{dH}{dt} + \left(\frac{\partial M}{\partial \sigma}\right)\frac{d\sigma}{dt},$$

(9)

where the field contribution arises from the application of the DC magnetic field H_0 and the stress contribution provides the sensing mechanism. It is noted that the field is applied at quasi-static speed (< 5 Hz).

2.1.1 Differential susceptibility

The model for the differential susceptibility $\partial M / \partial H$ is formulated through consideration of the energy lost when a ferromagnetic material is exposed to a cyclic magnetic field. As the field is applied, magnetic moments in the material rotate into the direction of the field, giving rise to the processes of domain wall motion and domain magnetization rotation. Domains rearrange so as to minimize the total energy, and as a consequence the magnetization changes.

In the idealized case of a defect-free material, on reversal of the field the magnetic moments return to their original orientations and the magnetization returns to its original value. In real engineering materials, however, defects such as crystal imperfections, cracks and voids are typically present which provide pinning sites to which domain walls attach since the total energy is lowest when pinning sites are intersected by a domain wall. For low magnetic field intensities about some equilibrium value, the domain walls remain pinned and bow reversibly, producing reversible magnetizations. But when the field intensity is sufficiently high so that the magnetic energy overcomes the pinning energy, domain walls detach irreversibly from the pinning sites and attach to remote sites. This mechanism produces energy losses which lead to magnetization hysteresis.

Assuming no other loss mechanisms, the energy supplied to a ferromagnetic material is either converted into magnetostatic energy (total magnetization) or dissipated in the form of irreversible magnetization changes (hysteresis loss due to domain wall pinning). This is formulated through an energy balance in which the total magnetization

178

is calculated from the difference between the maximum attainable magnetization energy, given by the anhysteretic condition, and the energy lost to pinning. The anhysteretic magnetization is calculated using a modified formulation of the Langevin equation [17], while the energy lost to pinning is calculated in terms of a pinning coefficient k that quantifies the density and strength of pinning sites in the material. It is noted that if there is no dissipation, the magnetization must necessarily follow the anhysteretic curve.

We first consider the anhysteretic magnetization M_{an}, which is quantified using the Langevin function $\mathcal{L}(z) \equiv \coth(z) - 1/z$, $-1 < \mathcal{L}(z) < 1$. As detailed in [17], M_{an} can be modeled by

$$M_{an} = M_s \, \mathcal{L}(He/a), \tag{10}$$

in which M_s is the saturation magnetization and the constant a, representing the effective domain density, is treated as a parameter to be estimated through a least squares fit to data or through adaptive parameter identification techniques. The effective magnetic field H_e is found from minimization of a suitable thermodynamic potential, and has the form

$$H_e = H + \alpha \, M + H_\sigma,$$

where H is the applied magnetic field, $\alpha \, M$ is the Weiss interaction field responsible for the alignment of neighboring magnetic moments within domains, and $H_\sigma \equiv (1/\mu_0) \left[\partial \left(\frac{3}{2} \sigma \varepsilon \right) / \partial M \right]$ is the field due to magnetoelastic interactions.

The differential equations for the irreversible M_{irr} and reversible M_{rev} components of magnetization ($M = M_{rev} + M_{irr}$) in the material can be shown to be [17]

$$M_{irr} = M_{an} - k \, \delta \, \frac{dM_{irr}}{dH_e} \tag{11}$$

$$M_{rev} = c \, (M_{an} - M_{irr}), \tag{12}$$

where the parameter δ is $+1$ when $dH / dt > 0$ and -1 when $dH / dt < 0$ to ensure that pinning losses always oppose the magnetization and c is a parameter that quantifies the amount by which domain walls bulge before breaking away from pinning sites.

The total magnetization is then dictated by the superposition of the irreversible and reversible contributions given by equations (11) and (12) respectively,

$$M = M_{irr} + M_{rev} = M_{an} - k \, \delta \, (1 - c) \, \frac{dM_{irr}}{dH_e}.$$

This equation leads to the total differential susceptibility $\partial M / \partial H$ upon differentiation and subsequent application of the chain rule. As detailed in [14], the total differential susceptibility has the form

$$\frac{\partial M}{\partial H} = (1 - c) \, \frac{M_{an} - M_{irr}}{\delta \, k - \widetilde{\alpha}(M_{irr}, \sigma) \, (M_{an} - M_{irr})} + c \, \frac{\partial M_{an}}{\partial H}. \tag{13}$$

It is noted that in equation (13), the parameter $\widetilde{\alpha}(M_{irr}, \sigma)$ represents an effective coupling coefficient which combines the interdomain coupling α and the magnetoelastic interactions,

$$\widetilde{\alpha}(M_{irr}, \sigma) = \alpha + \frac{3}{2 \, \mu_0} \, \frac{\partial^2 (\sigma \varepsilon)}{\partial M_{irr}^2}.$$

2.1.2 Magnetomechanical effect

We now consider the contribution of stress to the total magnetization, or magnetomechanical effect $\partial M / \partial \sigma$. A unifying description of the changes in magnetization due to the action of stress has been recently developed [18]. In the theory presented in [18] and implemented here, the main mechanism governing the magnetomechanical effect is the unpinning of domain walls produced upon application of the stress. On the basis of the key model assumption that hysteresis originates primarily from domain wall pinning, the freeing of domain walls from their pinning sites must cause the magnetization to change in such a way as to approach the anhysteretic magnetization.

Experimental measurements demonstrate that both the magnitude and the direction of stress-induced magnetization changes are profoundly influenced by the magnetic history of the specimen [18]. It has been observed that the

direction in which the magnetization changes with applied stress is independent of the sign of the stress, for small stresses and when the magnetization is sufficiently distant from the anhysteretic. It is then inferred that the direction of change is dependent not on the stress itself, but on a quantity which is independent of the sign of the stress. In this context, it has been hypothesized in [18] that this quantity is the elastic energy per unit volume, $W = \sigma^2/(2E)$, which is clearly independent of the sign of σ. The 'law of approach' to the anhysteretic condition is then formulated as follows: the rate of change of magnetization with elastic energy is proportional to the displacement of the prevailing magnetization from the anhysteretic magnetization, or $\partial M / \partial W \propto M - M_{an}$. The concept of the law of approach is now applied to the stress-induced magnetization of a magnetostrictive material.

As before, the law of approach may be modeled through irreversible and reversible components of the magnetization. It is noted that to a first approximation, the application of stress produces irreversible magnetization changes since ΔM arising from stress unloading is negligible. Thus, it is reasonable to formulate the law of approach in terms of the irreversible magnetization M_{irr},

$$\frac{\partial M_{irr}}{\partial W} = \frac{1}{\xi}\left(M_{an} - M_{irr}\right), \tag{14}$$

where ξ is a coefficient with dimensions of energy per unit volume that needs to be identified for magnetostrictive materials. Application of the chain rule $\partial M_{irr}/\partial W = (\partial M_{irr}/\partial \sigma)\,(\partial \sigma/\partial W)$ in equation (14), along with $\partial W / \partial \sigma = \sigma/E$, yields

$$\frac{\partial M_{irr}}{\partial \sigma} = \frac{\sigma}{E\,\xi}\left(M_{an} - M_{irr}\right). \tag{15}$$

A similar argument to that used in the field-induced case yields the reversible component,

$$\frac{\partial M_{rev}}{\partial \sigma} = c\left(\frac{\partial M_{an}}{\partial \sigma} - \frac{\partial M_{irr}}{\partial \sigma}\right). \tag{16}$$

It is noted that the reversibility coefficient c is the same as that defined in equation (12) because the energy available for domain wall bulging should be independent of the mechanism that produces the bulging, which can be either field- or stress-induced.

Summing the irreversible and reversible contributions given by equations (15) and (16) leads to

$$\frac{\partial M}{\partial \sigma} = (1 - c)\,\frac{\sigma}{E\,\xi}\left(M_{an} - M_{irr}\right) + c\,\frac{\partial M_{an}}{\partial \sigma}, \tag{17}$$

which quantifies the stress-induced magnetization of the magnetostrictive material.

It is noted that on application of stress the magnetization approaches a state of global energy equilibrium. This implies that the anhysteretic magnetization M_{an} must in this case be quantified by iteration of the Langevin function (10) until a solution which satisfies the equation identically is found. Further details regarding the differences between local and global solutions for equation (10) can be found in [14].

2.2 Magnetostriction

In order to quantify the contribution of stress to the magnetization given in (17), it is necessary to characterize the strain and stress states in the magnetostrictive material. To this end, it is necessary to consider first the deformations which occur in the material when the domain configuration changes. Several models exist for quantifying these deformations, including phenomenological formulations, quadratic laws for domain magnetization rotation, energy or thermodynamic formulations, elastomagnetic models, micromagnetic theories and magnetization rotation analysis. At low to moderate operating levels, or when material stresses are invariant, these deformations dominate over other material elastic dynamics. In such cases, it is theoretically possible to quantify the bulk magnetostriction upon knowledge of the domain configuration and the magnetostriction along easy crystallographic axes. In the case of Terfenol-D, nominal values for the latter are $\lambda_{111} = 1600 \times 10^{-6}$ and $\lambda_{100} = 90 \times 10^{-6}$, and $\lambda_s \approx 1000 \times 10^{-6}$. In practical terms, however, the domain configuration cannot be known in advance.

To motivate the approach employed here, we consider the particular case when the magnetic field is applied perpendicular to the axis in which the magnetic moments have been aligned by application of sufficiently large compression in the case of a polycrystalline material such as Terfenol-D, or perpendicular to the easy crystallographic

180

axis in a single crystal with uniaxial anisotropy. In either case domain rotation is the prevailing magnetization mechanism, and the magnetostriction along the field direction is given by [19]

$$\lambda(M) = \frac{3}{2} \lambda_s \left(\frac{M}{M_s} \right)^2, \tag{18}$$

which predicts a quadratic relation between λ and M. Equation (18) is a single-valued functional, while extensive experimental evidence demonstrates that the λ-M relationship exhibits some degree of hysteresis. For transducer modeling purposes, it is feasible to utilize a single valued λ-M functional to model the overall shape and to let M provide the hysteresis through the hysteretic mechanisms in M-H.

It should be noted that equation (18) is not sufficiently general when domain wall motion is significant, such as when the operating stress acting on the Terfenol-D material is not extreme ($\sigma_0 < -6.9$ to -20.7 MPa). In order to provide a more general magnetostriction model, we consider a series expansion symmetric about $M = 0$,

$$\lambda(M) = \sum_{i=0}^{\infty} \gamma_i M^{2i},$$

in which the coefficients γ_i need to be identified from experimental data. It is noted that quadratic relation (18) is achieved for $i = 1$ with $\gamma_0 = 0$ and $\gamma_1 = (3 \lambda_s)/(2 M_s^2)$. For implementation purposes, we consider in this study a quartic law in which the series is truncated after $i = 2$,

$$\lambda(M) = \gamma_1 M^2 + \gamma_2 M^4. \tag{19}$$

2.3 Elastic Strains

The magnetostriction λ given by equation (19) quantifies the reorientation of magnetic moments towards the direction of applied bias magnetization H_0. It was shown in [20] that this magnetostriction is a generalization of the term dH in linear models. It ignores, however, the elastic properties of the magnetostrictive material as it vibrates, as represented in the linear models by $(1/E^H)\Delta\sigma$. In this section, a PDE system is formulated which models the elastic response of the magnetostrictive material and relevant transducer components located in the load path. The input to this PDE is formulated through the magnetostriction λ and the external forces F_{ext} acting on the transducer. The solution to the PDE is the longitudinal displacements $u(t, x)$ relative to the prestressed position.

The structural dynamics are modeled through consideration of the magnetostrictive rod, prestress bolt, prestress washer, and mass load as depicted in Figure 4. The prestress bolt provides a stress $\sigma_0 < 0$ by compressing the magnetostrictive rod against the washer, modeled by a linear spring k_L and dashpot c_L. The rod is assumed to have length L, cross sectional area A, and longitudinal coordinate x. The material density is ρ, the elastic modulus is E, the internal (Kelvin-Voigt) damping is c_D, and the external load is modeled by a point mass m_L. It should be noted that parameter E lies between the elastic modulus at constant H, E^H, and at constant B, E^B. Since E^H and E^B depend upon the field intensity, so does E. However, for simplicity E is treated as a nominal material stiffness.

Assuming linear elasticity and small displacements, force balancing yields the wave equation for the rod vibrations,

$$\rho \frac{\partial^2 u}{\partial t^2}(t, x) = \frac{\partial \sigma}{\partial x}(t, x). \tag{20}$$

Here, the stress at cross sections x in the rod is given by [20]

$$\sigma(t, x) = E \frac{\partial u}{\partial x}(t, x) + c_D \frac{\partial^2 u}{\partial x \partial t}(t, x) - E \lambda(t, x) + \sigma_0, \tag{21}$$

where λ is given by (19) and σ_0 is the applied prestress. When integrated over a cross section, equation (21) yields the total inplane resultant N ($N > 0$ in tension, $N < 0$ in compression),

$$N(t, x) = E A \frac{\partial u}{\partial x}(t, x) + c_D A \frac{\partial^2 u}{\partial x \partial t}(t, x) - E A \lambda(t, x) + A \sigma_0.$$

To obtain appropriate boundary conditions, it is first noted that at the fixed end of the rod $u(t, x) = 0$. At the end $x = L$, force balancing over an infinitesimal cross section of the rod yields [20]

$$N(t, L) = -m_L \frac{\partial^2 u}{\partial t^2}(t, L) - c_L \frac{\partial u}{\partial t}(t, L) - k_L u(t, L) - F_{ext}(t), \tag{22}$$
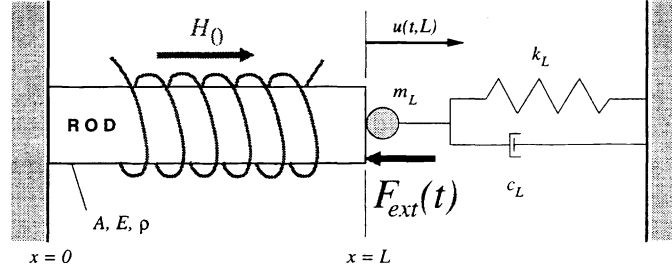
Figure 4: Simulation setup corresponding to the transducer of Figure 3. The external force F_{ext} pertains to operation of the transducer in sensor mode.

where F_{ext} is the force due to the load. The negative sign implies that $F_{ext} > 0$ produces a compressive force.

For implementation purposes, the model is formulated in weak or variational form by multiplying the strong form by test functions ϕ followed by integration throughout the length of the rod. This reduces the smoothness requirements on the finite element basis since displacements and test functions need to be differentiated only once compared to the second derivatives present in the strong form. The space of test functions is $V = H_L^1(0, L) \equiv \{\phi \in H^1(0, L) \mid \phi(0) = 0\}$, so that for all $\phi(x) \in V$,

$$\int_0^L \rho A \frac{\partial^2 u}{\partial t^2}(t, x) \phi(x)\, dx = -\int_0^L \left[c_D A \frac{\partial^2 u}{\partial x \partial t}(t, x) + E A \frac{\partial u}{\partial x}(t, x) - E A \lambda(t, x) \right] \frac{\partial \phi}{\partial x}(x)\, dx$$

$$- \left[m_L \frac{\partial^2 u}{\partial t^2}(t, L) + c_L \frac{\partial u}{\partial t}(t, L) + k_L\, u(t, L) + F_{ext}(t) \right] \phi(L). \tag{23}$$

The solution $u(t, x)$ to this equation defines the longitudinal displacements about the prestressed position and completely defines the elastic state through the strain, given by $\varepsilon(t, x) = \partial u\, /\, \partial x(t, x)$, and the stress $\sigma(t, x)$, given by equation (21). Finally, the accelerations are computed from equation (20).

3 MODEL RESULTS

In this section, the magnetomechanical transducer model is employed to characterize stiffness changes associated with DC magnetic fields applied to the transducer of Figure 3. The magnetostrictive driver is 115 mm (4.53 in) long by 12.7 mm (0.5 in) in diameter. In order to take advantage of the optimized model parameters identified previously [15, 16], it is assumed that the magnetostrictive material is monolithic Terfenol-D of composition $Tb_{.28}Dy_{.72}Fe_{1.92}$ manufactured by the modified Bridgman process.

The numerical procedure employed for the simulations is described as follows. First, the magnetostrictive rod is precompressed to a value $\sigma_0 = -10.35$ MPa (-1.5 ksi). Assuming an initial demagnetized state ($M = 0$), the model rod is then magnetized with a slowly-varying magnetizing field of amplitude H_0 and ensuing magnetization M_0, which once reached is thereafter held constant. It is noted that in experiments, the sample is demagnetized at constant stress by applying a decaying-amplitude sinusoidal magnetic field of initial amplitude sufficiently large to ensure that a state of saturation magnetization is achieved. For Terfenol-D, a typical demagnetization signal under the indicated prestress will have an initial amplitude of 160 kA/m or more, and the decay rate will be 80 (A/m)/cycle or less. The magnetization values employed in the simulations are shown in Figure 5 and labeled as points 1-8.

The second step consists of applying a simulated impact force at $x = L$, which by virtue of the magnetomechanical effect produces a magnetization change in the magnetostrictive rod. The peak value employed was $\max(F_{ext}) = 1000$ N (224 lb). The rod displacements and corresponding strains and accelerations are then computed in the third step. The strain and acceleration responses corresponding to bias point 1 are shown in Figure 6(a)-(b). The resulting f_r versus H_0 plot is shown in Figure 7.

It is pointed out that the simulated ΔE effect is negative in the region of low bias fields and positive in the region of medium to high bias fields, which is in agreement with the trends observed in the experimental data of Figure 2(b). The maximum frequency shift predicted by the model occurs between points 3-8 (1344-1481 Hz), which corresponds to a stiffness increase of 21%, while the frequency shift between points 1-8 (1391-1481 Hz) corresponds to a stiffness
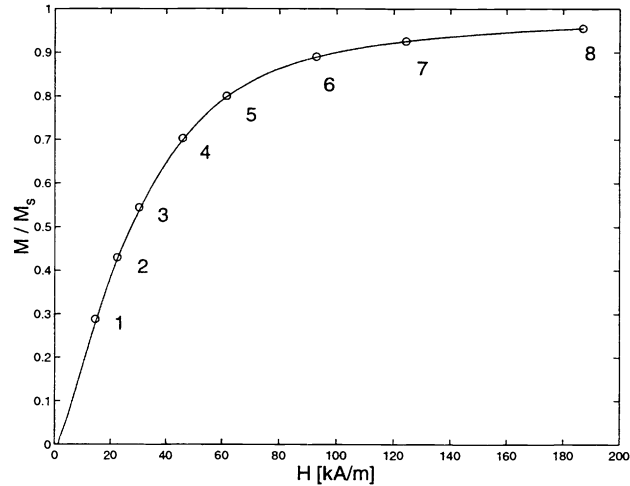
182

Figure 5: Initial magnetization curve showing the bias magnetization values employed in the simulations, points 1-8. The eight bias points correspond to the pairs (H_0, M_0), in kA/m: Pt. 1, (14.4,220.8); Pt. 2, (23.9,349.6); Pt. 3, (30.2,416.3); Pt. 4, (45.9,537.4); Pt. 5, (61.6,612.0); Pt. 6, (93.0,680.9); Pt. 7, (124.3,708.0); Pt. 8, (186.9,730.6). $M_s = 765$ kA/m.
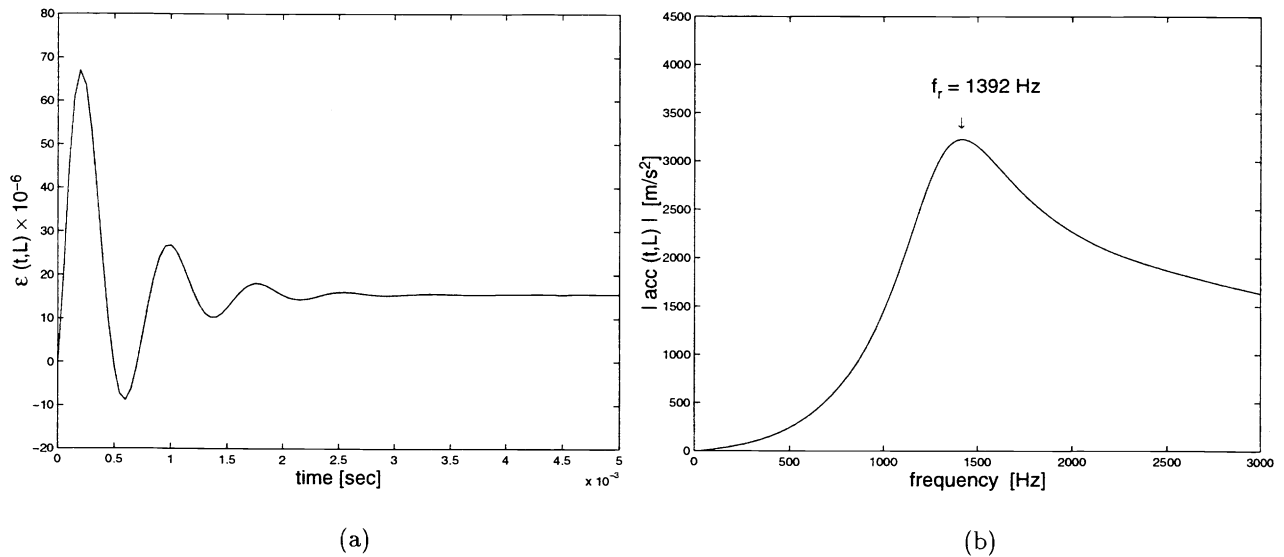

(a)

(b)

Figure 6: (a) Modeled strain response and (b) acceleration response corresponding to bias point 1.

increase of 13%. This stiffness increase is substantially smaller than the giant effects of up to 200% indicated in Figure 2(b) for the prestress range under consideration. It is emphasized that the parameters employed for the simulations, indicated in Table 1, had been optimized from magnetization and strain data and thus may not reflect optimal model performance for the stiffness. Because of the presence of several local minima in the penalty function employed for optimization of parameters, the determination of a unique, physically-consistent set of model parameters is quite complicated. In addition, model results are highly sensitive to variations in certain parameters, especially the parameter ξ which quantifies the rate of approach to M_{an} with stress. Work is in progress to gather the necessary experimental data on stiffness changes of Terfenol-D under varied bias conditions.

Finally, while the model addresses dynamic elastic effects through the wave equation, frequency dependencies in the magnetic system such as those associated with eddy currents have not been considered. A formulation for the magnetization dynamics similar to that employed in [2] is in process of implementation for this particular problem.
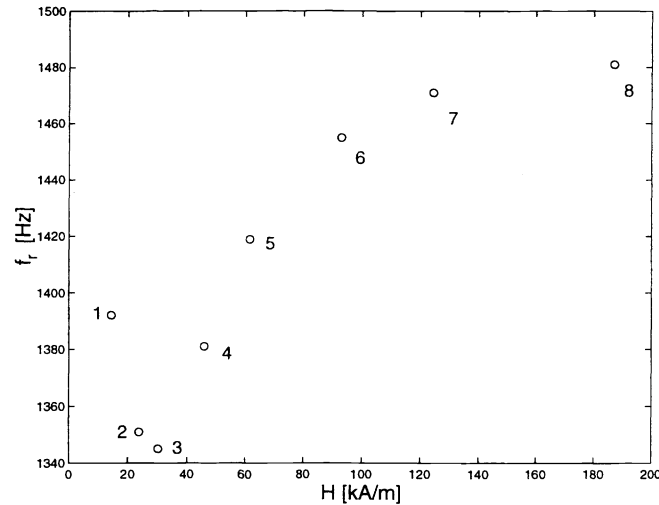
183

Figure 7: Modeled frequency shift produced by DC magnetic fields, points 1-8.

Magnetization	Magnetostriction	Structural	Load	Geometry
$a = 6500$ A/m	$M_0 = 0.8 \times 10^6$ A/m	$E = 30 \times 10^9$ Pa	$k_L = 2.5 \times 10^6$ N/m	$L = 0.115$ m
$k = 6000$ A/m	$\lambda_s = 1000 \times 10^{-6}$	$\rho = 9250$ kg / m^3	$m_L = 0.5$ kg	$D = 0.0127$ m
$c = 0.008$	$\gamma_1 = 2.9 \times 10^{-15}$ m^2/A^2	$c_D = 1 \times 10^6$ Ns/m	$c_L = 1 \times 10^3$ Ns/m	
$\alpha = 0.03$	$\gamma_2 = -7.5 \times 10^{-28}$ m^4/A^4			
$M_s = 0.765 \times 10^6$ A/m				
$\xi = 24.5 \times 10^3$ Pa				

Table 1: Physical parameters and dimensions used in the coupled elastic-magnetic model.

4 CONCLUDING REMARKS

This paper was motivated by the need for fundamental models of the stiffness changes occurring in magnetostrictive transducers in response to DC or bias magnetic fields. A magnetomechanical model was presented and employed to characterize the resonance frequency shifts occurring in a typical magnetostrictive transducer upon variation of the bias field. The model transducer consisted of a cylindrical magnetostrictive driver, a surrounding excitation solenoid, a magnetic circuit and a prestress mechanism. The model was constructed in three steps. In the first step, the magnetization was assumed due to a slowly varying magnetic field and a magnetomechanical component associated with the stresses in the magnetostrictive driver. The magnetization model was then constructed by considering the energy dissipated when domain walls attach to and detach from inclusions in the material. In the second step, the magnetostriction was formulated in terms of the magnetization by considering an even-terms series expansion symmetric about $M = 0$. The elastic response was modeled in the last step through a wave equation formulated in weak form, yielding a PDE with inputs given by the magnetostriction and the external loading, and boundary conditions given by the specific transducer design.

The results obtained with the model agree qualitatively with published trends on the ΔE effect. The predicted ΔE effect is an order of magnitude smaller than that observed in free-standing samples at the same preload ($\sigma_0 = -10.35$ MPa). Work is in progress to gather the necessary experimental data needed for identification of parameters capable of providing optimal fits to magnetization, strain *and* stiffness data. Of particular interest is the quantification of the approach parameter ξ for Terfenol-D.

ACKNOWLEDGMENTS

184

REFERENCES

[1] R. C. Smith, "Inverse compensation for hysteresis in magnetostrictive transducers," CRSC Technical Report CRSC-TR98-36, 2000 and *Mathematical and Computer Modeling*, to appear.

[2] J. Slaughter, M. J. Dapino, R. C. Smith and A. B. Flatau, "Modeling of a Terfenol-D transducer," in *Proc. of SPIE, Smart Structures and Materials 2000*, Vol. 3985-38, Newport Beach, CA, 2000.

[3] A. B. Flatau, M. J. Dapino and F. T. Calkins, "High-bandwidth tunability in a smart vibration absorber," in *Proc. of SPIE Smart Structures and Materials*, Vol. 3327, pp. 463–473, San Diego, CA, 1998.

[4] A. E. Clark, *Ferromagnetic materials*, Vol. 1, Ch. 7, pp. 531–589, E. P. Wohlfarth, Ed., North Holland Publishing, Co., Amsterdam, 1980.

[5] A. E. Clark, J. B. Restorff and M. Wun-Fogle, "Magnetoelastic coupling and ΔE effect in $Tb_x Dy_{1-x}$ single crystals," *J. Appl. Phys.*, **73**(10), pp. 6150–6152, May 1993.

[6] F. Calkins and A. Flatau, "Transducer based measurements of Terfenol-D material properties," in *Proc. of SPIE, Symposium on Smart Structures and Materials*, Vol. 2717, pp. 709–719, San Diego, CA, 1996.

[7] H. Savage, A. Clark and J. Powers, "Magnetomechanical coupling and ΔE effect in highly magnetostrictive rare earth-Fe_2 compounds," *IEEE Trans. Magn.*, **MAG-11**, pp. 1355–1357, September 1975.

[8] N. W. Hagood and A. von Flotow, "Damping and structural vibrations with piezoelectric materials and passive electrical networks," *Journal of Sound and Vibration*, **146**, pp. 243–268, 1991.

[9] A. E. Clark and H. T. Savage, "Giant magnetically induced changes in elastic moduli in $Tb_{.3}Dy_{.7}Fe_2$," *IEEE Trans. on Sonics and Ultrasonics*, **SU-22**, pp. 50–52, January 1975.

[10] F. T. Calkins, M. J. Dapino and A. B. Flatau, "Effect of prestress on the dynamic performance of a Terfenol-D transducer," in *Proc. of SPIE, Smart Structures and Materials*, Vol. 3041, pp. 293–304, San Diego, CA, 1997.

[11] J. Hudson, S. C. Busbridge and A. R. Piercy, "Magnetomechanical coupling and elastic moduli of polymer-bonded Terfenol," *J. Appl. Phys.*, **83**, pp. 7255–7257, June 1998.

[12] J. B. Restorff, M. Wun-Fogle and A. E. Clark, "Piezomagnetic properties, saturation magnetostriction and ΔE effect in DyZn at 77K," *J. Appl. Phys.*, **83**, pp. 7288–7290, June 1998.

[13] F. T. Calkins, *Design, analysis and modeling of giant magnetostrictive transducers*, Ph.D. dissertation, Iowa State University, Ames, Iowa, 1997.

[14] M. J. Dapino, *Nonlinear and hysteretic magnetomechanical model for magnetostrictive transducers*, Ph.D. dissertation, Iowa State University, Ames, Iowa, 1999.

[15] M. J. Dapino, R. C. Smith, L. E. Faidley and A. B. Flatau, "A coupled structural-magnetic strain and stress model for magnetostrictive transducers," *J. of Intell. Mater. Syst. and Struct.*, submitted 9/99, and CRSC Technical Report CRSC-TR99-24.

[16] M. J. Dapino, F. T. Calkins, R. C. Smith and A. B. Flatau, "A magnetoelastic model for magnetostrictive sensors," in *Proc. of ACTIVE 99*, S. Douglas, Ed., Vol. 2, pp. 1193–1204, INCE USA, 1999.

[17] D. C. Jiles and D. L. Atherton, "Theory of ferromagnetic hysteresis," *J. Magn. Magn. Mater.*, **61**, pp. 48–60, 1986.

[18] D. C. Jiles, "Theory of the magnetomechanical effect," *J. Phys. D: Appl. Phys.*, **28**, pp. 1537–1546, 1995.

[19] B. D. Cullity, *Introduction to magnetic materials*, Addison-Wesley, Reading, Massachusetts, 1972.

[20] M. J. Dapino, R. C. Smith and A. B. Flatau, "A structural-magnetic strain model for magnetostrictive transducers," *IEEE Trans. Magn.*, to appear.